18. M. R. Ruiz, S. K. Leggett, F. Allard, *ibid.* **491**, L107 (1997).
19. X. Delfosse *et al.*, *Astron. Astrophys.* **327**, L25 (1997).
20. C. Beichman *et al.*, paper presented at the Very Low-Mass Stars and Brown Dwarfs in Stellar Clusters and Associations Euroconference, La Palma, Spain, 11 to 15 May 1998.
21. C. F. Prosser, J. R. Stauffer, R. P. Kraft, *Astron. J.* **101**, 1361 (1991).
22. E. L. Martín, R. Rebolo, A. Magazzú, *Astrophys. J.* **436**, 262 (1994).
23. E. Polomski, S. Vennes, J. R. Thorstensen, M. Mathioudakis, E. E. Falco, *ibid.* **486**, 179 (1997).
24. M. Lampton *et al.*, *Astrophys. J. Suppl.* **108**, 545 (1997).
25. G. Basri and E. L. Martín, *Astrophys. J.*, in press.
26. E. L. Martín *et al.*, *ibid.* **499**, L61 (1998).
27. G. Chabrier, I. Baraffe, B. Plez, *ibid.* **459**, L91 (1996).
28. M. S. Bessell, F. Castelli, B. Plez, *Astron. Astrophys.* **333**, 231 (1998).
29. A. Burrows *et al.*, *Asp. Conf. Ser.* **134**, 354 (1998).
30. I. Baraffe, G. Chabrier, F. Allard, P. H. Hauschildt, *Astron. Astrophys.*, **337**, 403 (1998).
31. D. Saumon *et al.*, *Astrophys. J.* **460**, 993 (1996).
32. P. Artymowicz, *Asp. Conf. Ser.* **134**, 152 (1998).
33. P. Bodenheimer, *ibid.*, p. 115.
34. F. Bruhweiler *et al.*, *Bull. Am. Astron. Soc.* **191**, 47.03 (1997).
35. M. Mayor and D. Queloz, *Nature* **378**, 355 (1995).
36. G. Marcy, *ibid.* **391**, 127 (1998).
37. We thank N. González Pérez for assistance with the infrared observations at the TCS, J. Casares and I. Martínez-Pais for their assistance at the INT, I. Baraffe and the Lyon group for providing us with new evolutionary models for very low masses before publication, E. Polomski for sending the published spectrum of G 196-3 in digitalized format, and E. L. Martín and G. Basri for sharing data before publication. This paper is based on observations made with the IAC80; the European Space Agency's OGS and the TCS, operated by the Instituto de Astrofísica de Canarias (IAC) at the OT; and the NOT, the INT, and the WHT, operated on the island of La Palma by the Isaac Newton Group at the ORM of the IAC. Partial financial support was provided by the Spanish Direccion General de Enseñanza Superior, project no. PB95-1132-C02-01.

7 August 1998; accepted 8 October 1998

Requirement for MAPK Activation for Normal Mitotic Progression in *Xenopus* Egg Extracts

Thomas M. Guadagno and James E. Ferrell Jr.*

The p42 mitogen-activated protein kinase (MAPK) is required for progression through meiotic M phase in *Xenopus* oocytes. This report examines whether it also plays a role in normal mitotic progression. MAPK was transiently activated during mitosis in cycling *Xenopus* egg extracts after activation of the cyclin-dependent kinase Cdc2–cyclin B. Interference with MAPK activation by immunodepletion of its activator MEK, or by addition of the MEK inhibitor PD98059, caused precocious termination of mitosis and interfered with production of normal mitotic microtubules. Sustained activation of MAPK arrested extracts in mitosis in the absence of active Cdc2–cyclin B. These findings identify a role for MEK and MAPK in maintaining the mitotic state.

Mitosis is initiated by the activation of Cdc2–cyclin complexes. In *Xenopus* egg extracts, three mitotic Cdc2–cyclin complexes have been identified; they are activated and inactivated sequentially, beginning with Cdc2–cyclin A1, followed by Cdc2–cyclin B1, and finally Cdc2–cyclin B2 (*1*). The last of the three, Cdc2–cyclin B2, is inactivated just after nuclear envelope breakdown (NEBD) (*1*). Chromatin condensation and NEBD persist throughout the remainder of M phase in the absence of active Cdc2. This persistence could be the result of slow reversal of the effects of Cdc2, or these aspects of mitosis could be actively maintained by some regulatory protein other than Cdc2.

Several lines of evidence raise the possibility that p42 MAPK (also called ERK2) participates in mitosis. MAPK activation is required for *Xenopus* oocyte maturation, and the regulation of oocyte maturation and is similar to regulation of mitosis in many important respects (*2*). Moreover, in sea urchin embryos (*3*), mammalian cell lines (*4*), and cycling *Xenopus* egg extracts (Figs. 1C; 2C; and 3, A and C) (*5, 6*), MAPKs are activated during mitosis. Finally, MAPKs have been implicated in the spindle assembly checkpoint in extracts and in a *Xenopus* cell line (XTC-2) (*5–7*), and there is precedent for proteins involved in this checkpoint to be involved in establishing the timing of an unperturbed mitosis (*8*). However, depletion of p42 MAPK or inhibition of p42 MAPK activation has no effect on the activation or inactivation of Cdc2 in cycling *Xenopus* egg extracts, which suggests that p42 MAPK might be dispensable for mitotic entry and exit (*5*).

We examined the role of p42 MAPK in mitosis in cycling extracts, monitoring not only Cdc2 activation and inactivation but also the main morphological hallmarks of mitosis—nuclear envelope breakdown, chromatin condensation, and microtubule dynamics. We prevented mitotic activation of p42 MAPK in cycling extracts by one of two treatments that inhibit MEK, the protein kinase that phosphorylates and activates MAPK: addition of the MEK inhibitor PD98059 (*9*) or immunodepletion of MEK (*10*). Both approaches blocked p42 MAPK activation (Fig. 1, A and C). We then tested whether Cdc2 activity cycled normally in the absence of MAPK activation. Activation and inactivation of Cdc2 was similar in control and in PD98059-treated extracts and in mock-depleted and MEK-depleted extracts (Fig. 1, B and D), in agreement with previous reports (*5*).

We also tested whether nuclear envelope breakdown and re-formation and chromatin condensation and decondensation were altered in the absence of MAPK activation (*11*). We added low concentrations of demembranated sperm (500 per microliter) (*12*) to MAPK-inhibited and control cycling extracts, allowed nuclei to form, and took portions at various times to assess chromatin condensation by 4′,6-diamidino-2-phenylindole (DAPI) staining and NEBD by phase-contrast microscopy. Both the control and PD98059-treated extracts underwent chromatin condensation and nuclear envelope breakdown 50 min after cycling was initiated (Fig. 2, A and B). However, the extracts in which MEK was inhibited exited mitosis prematurely (Fig. 2, A and B). The chromatin had decondensed and nuclear envelopes reformed by 60 min in the PD98059-treated extract but not until 75 min in the control extract. Thus the duration of mitosis (taken here to be the interval between NEBD and re-formation) in the MEK-inhibited extract was less than half that in the control extract. Premature mitotic exit was also observed with MEK-depleted extracts but not with mock-depleted extracts (Fig. 2C), and adding purified recombinant MEK to the MEK-depleted extracts restored mitosis to a normal length (Fig. 2D). These results indicate that MEK activation is necessary to maintain the mitotic state for a normal period of time. Because p42 and p44 MAPK are the only known substrates of MEK, and only p42 is present in egg extracts, these findings implicate p42 MAPK in maintenance of the mitotic state.

When MAPK is artificially activated before Cdc2 is activated, it can inhibit cyclin degradation and hence prolong Cdc2 activa-

Department of Molecular Pharmacology, Stanford University School of Medicine, Stanford, CA 94305–5332, USA.

*To whom correspondence should be addressed. E-mail: ferrell@cmgm.stanford.edu

tion and mitosis (*13*). However, the present results (Figs. 1 and 2) suggest that p42 MAPK may be able to sustain mitosis even after Cdc2 is inactivated. To test this idea further, we established conditions for inducing sustained activation of p42 MAPK in a cycling extract at about the time when transient MAPK activation normally occurs. We activated MEK and MAPK in the extract by adding recombinant malE-Mos (*14*), a MEK kinase, and timed the Mos addition to be too late to prevent cyclin destruction (Fig. 3, A and B).

Under these circumstances Mos treatment had no effect on the timing of Cdc2 activation (Fig. 3B), NEBD (Fig. 3C), or chromatin condensation (Fig. 3D), all of which occurred by 60 min in both control and Mos-treated cycling extracts. Moreover, Cdc2 inactivation occurred normally in both control and Mos-treated extracts (Fig. 3B). The inactivation of Cdc2 coincided with mitotic cyclin degradation as determined by [^{35}S]methionine labeling, gel electrophoresis, and autoradiography (*15*).

Control extracts returned to interphase by 80 min, as indicated by decondensed chromatin and intact nuclear envelopes (Fig. 3, C and D). In contrast, Mos-treated extracts remained arrested in mitosis for the duration of the experiment despite their lack of Cdc2 activity (Fig. 3, C and D). Thus, active p42 MAPK can maintain the mitotic state in the absence of active Cdc2–cyclin B. This finding implies a role for p42 MAPK in maintaining mitosis and indicates that inactivation of p42 MAPK may be required for exit from mitosis.

The p42 MAPK associates with microtu-

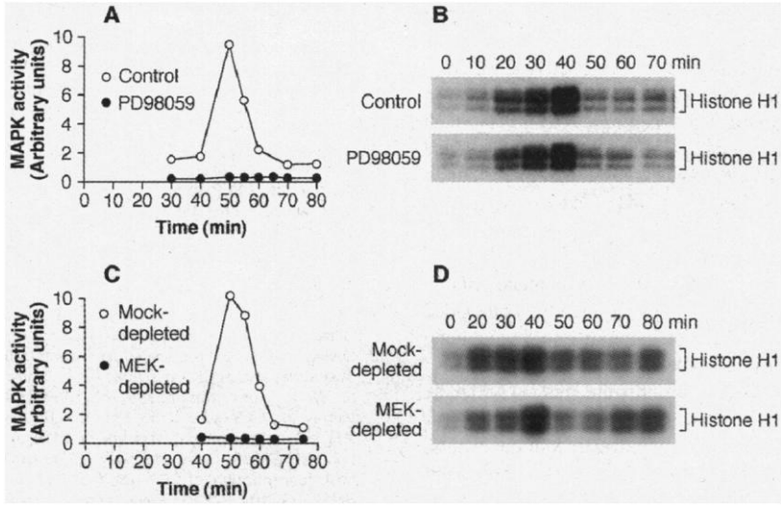

Fig. 1. Normal activation and inactivation of Cdc2 in extracts after inhibition or immunodepletion of MEK. (**A** and **B**) Effects of MEK inhibitor PD98059 on MAPK activation and Cdc2 activity. Extracts were treated with PD98059 or DMSO (*8*). (**C** and **D**) Effects of MEK immunodepletion on MAPK activation and Cdc2 activity. Extracts were depleted of MEK with antibody 662 or were mock-depleted with rabbit IgG (*8*) and warmed to room temperature to initiate cycling. The resulting MAPK activity was assessed by immune complex kinase assay (A and C), and Cdc2 activity was assessed with histone H1 as substrate (B and D). Indicated times are relative to initiation of cycling.

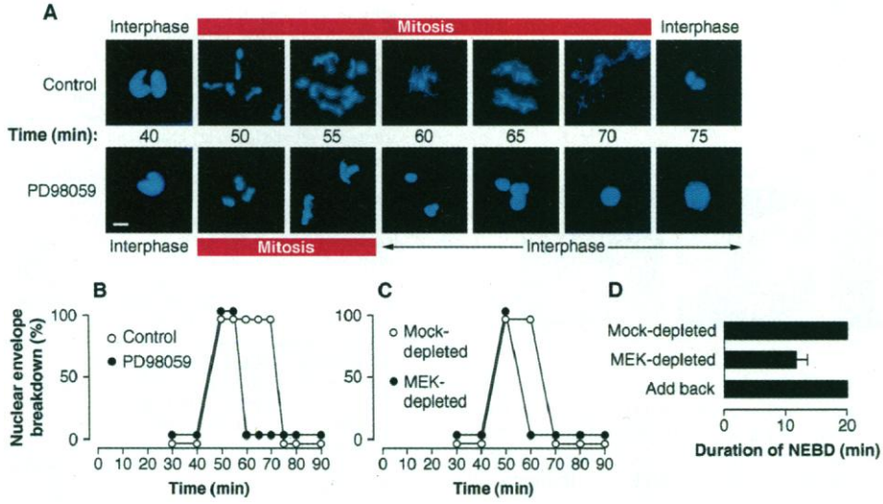

Fig. 2. Premature mitotic exit after inhibition of MEK. (**A**) Nuclear morphology in control and PD98059-treated extracts. Nuclei were stained with DAPI and observed by fluorescence microscopy. Scale bar, 20 μm. (**B**) NEBD in control DMSO-treated extracts and PD98059-treated extracts. (**C**) NEBD mock-depleted and MEK-depleted extracts. (**D**) Restoration of normal mitotic duration in MEK-depleted extracts supplemented with recombinant MEK. Data are averages from two (add back) or three (mock-depleted, MEK-depleted) experiments. Error bar represents one standard deviation for the MEK-depleted extracts. For other extracts the duration of mitosis did not vary measurably from experiment to experiment. NEBD was assessed by phase-contrast microscopy. In (A) through (C), indicated times are relative to initiation of cycling.

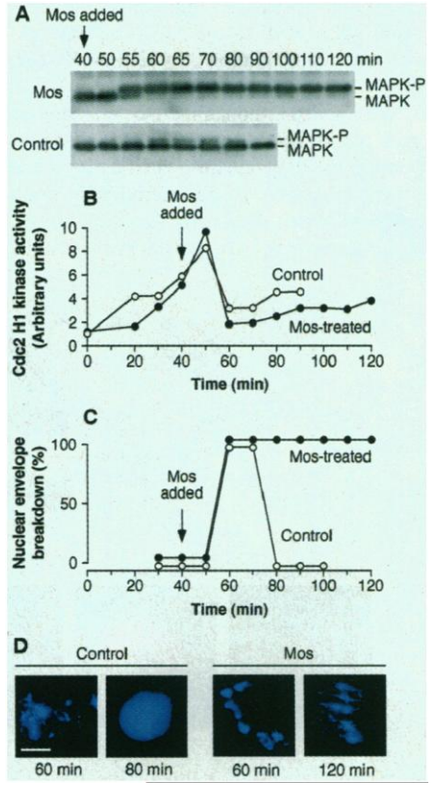

Fig. 3. Effect of prolonged mitotic activation of MAPK on Cdc2 activity and mitotic exit. Recombinant malE-Mos (a Mos–maltose-binding protein fusion protein; 300 nM final concentration) or buffer was added to cycling *Xenopus* egg extracts 40 min after initiation of cycling. (**A**) MAPK immunoblot. Lower band represents nonphosphorylated MAPK. Upper band represents phosphorylated MAPK. (**B**) Cdc2 H1 kinase activity. (**C**) NEBD assessed by phase-contrast microscopy. (**D**) Chromatin condensation, assessed by DAPI staining and fluorescence microscopy. Scale bar, 20 μm. Indicated times are relative to initiation of cycling.

bules (*16*) and in particular with the mitotic spindle (*3, 4, 7*). We therefore examined whether microtubule dynamics were altered in cycling extracts in which MEK was inhibited. We prepared cycloheximide-treated interphase egg extracts devoid of cyclins A1, B1, and B2 (*17*) and mock-depleted them, immunodepleted them of MEK, or immunodepleted them and then added back purified recombinant MEK R4F (an activated form of human MEK) (*18*) to yield a physiological concentration of MEK (Fig. 4A). We then drove the extracts into a stable mitotic state by addition of purified nondegradable sea urchin cyclin B. This yielded large amounts of Cdc2–cyclin B activity in all three types of extracts (Fig. 4B). The active Cdc2–cyclin B brought about activation of p42 MAPK in the mock-depleted extract (Fig. 4B, lane 2), demonstrating that p42 MAPK can be activated downstream of Cdc2–cyclin B in this system. MEK depletion blocked Cdc2–cyclin B-induced activation of p42 MAPK, and adding back recombinant MEK R4F to the MEK-depleted extract restored activation of p42 MAPK (Fig. 4B).

We added rhodamine-labeled bovine brain tubulin and demembranated *Xenopus* sperm to the three cyclin-treated extracts and assessed the size of the microtubule asters nucleated from the sperm centrioles (*19*). Larger microtubule asters were present in the MEK-depleted mitotic extracts than in the mock-depleted extract, despite the fact that both extracts had high levels of Cdc2 activity (Fig. 4C). Mitotic extracts treated with the MEK inhibitor PD98059 also produced large asters (*15*). The addition of purified recombinant MEK protein to MEK-depleted extracts restored production of normal small mitotic asters (Fig. 4C). Taken together, these data indicate that p42 MAPK activity is required for normal mitotic microtubules.

To determine whether MAPK activation was sufficient to produce mitotic microtubule asters in the absence of Cdc2 activity, we compared microtubule asters in interphase extracts and Mos-treated interphase extracts (which contain high p42 MAPK activity and low Cdc2 activity). Both extracts supported the formation of large asters (Fig. 4D), and extensive networks of microtubules could be seen in the absence of sperm in both extracts. Thus MAPK activation is not sufficient to initiate mitotic microtubule dynamics. Evidently, both Cdc2 and MAPK function in initiating or maintaining mitotic microtubules (*20*).

Our results demonstrate that p42 MAPK is activated downstream of Cdc2 during mitosis in *Xenopus* egg extracts, that the mitotic state is actively maintained during the period after Cdc2 inactivation, and that p42 MAPK activity is essential for this maintenance. During meiosis in oocytes, p42 MAPK has a similar function, suppressing a return to interphase during the interval between meiosis I and meiosis II (*21, 22*). Thus this versatile, evolutionarily ancient protein kinase, implicated in diverse responses to extracellular signals, is also an important component of the cell cycle clock.

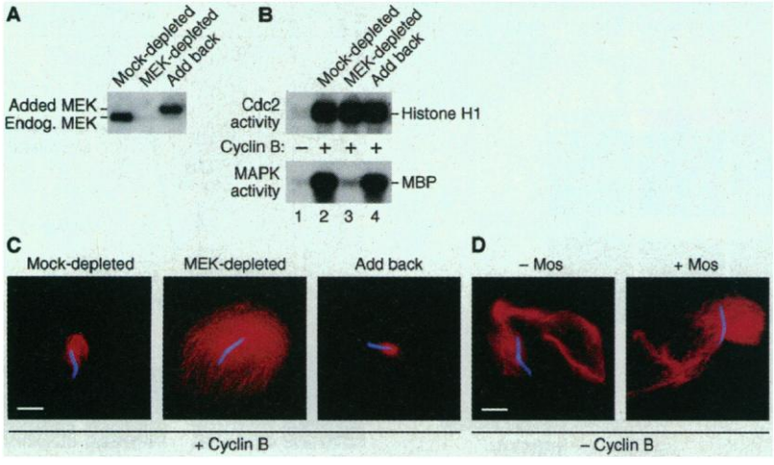

Fig. 4. Effect of MEK inhibition on aster formation. Mock-depleted or MEK-depleted interphase extracts were prepared from electrically activated cycloheximide-treated eggs and were treated with nondestructible sea urchin Δ90 cyclin B (to drive them into a stable mitotic state) or with no cyclin (to keep them in interphase). (**A**) Amounts of MEK in a mock-depleted extract, a MEK-depleted extract, and a MEK-depleted extract supplemented with human MEK R4F. Immunoblot with an antiserum (662) raised against a peptide that is identical in the *Xenopus* and human MEK proteins. (**B**) Cdc2 H1 kinase activity (upper autoradiogram) and MAPK immune complex kinase activity (lower autoradiogram) in an interphase extract (lane 1); a mock-depleted, mitotic extract (lane 2); a MEK-depleted, mitotic extract (lane 3); and a MEK-depleted mitotic extract supplemented with MEK R4F (lane 4). (**C**) Sperm-nucleated aster formation in mitotic Δ90 cyclin B–treated extracts with or without normal MAPK activity. A mock-depleted extract (left), MEK-depleted extract (center), and MEK-depleted extract supplemented with MEK R4F (right) are shown. DAPI staining of the sperm is shown in blue; rhodamine-labeled tubulin is shown in red. Scale bar, 20 μm. (**D**) Long interphase-like microtubules in interphase extracts with normal low MAPK activity (left) or high MAPK activity induced by Mos (right). Scale bar, 20 μm.

References and Notes

1. J. Minshull, R. Golsteyn, C. S. Hill, T. Hunt, *EMBO J.* **9**, 2865 (1990).
2. N. Sagata, *BioEssays* **19**, 13 (1997).
3. S. Chiri, C. De Nadai, B. Ciapa, *J. Cell Sci.* **111**, 2519 (1998); R. Philipova and M. Whitaker, *ibid.*, p. 2497 (1998).
4. P. S. Shapiro *et al.*, *J. Cell Biol.* **142**, 1533 (1998); M. Zecevic *et. al.*, *ibid.*, p. 1547 (1998).
5. K. Takenaka, Y. Gotoh, E. Nishida, *ibid.* **136**, 1091 (1997); D. A. Cross and C. Smythe, *Exp. Cell Res.* **241**, 12 (1998).
6. J. Minshull, H. Sun, N. K. Tonks, A. W. Murray, *Cell* **79**, 475 (1994); K. Takenaka, T. Moriguchi, E. Nishida, *Science* **280**, 599 (1998).
7. X. M. Wang, Y. Zhai, J. E. Ferrell Jr., *J. Cell Biol.* **137**, 433 (1997).
8. S. S. Taylor and F. McKeon, *Cell* **89**, 727 (1997); G. J. Gorbsky, R. H. Chen, A. W. Murray, *J. Cell Biol.* **141**, 1193 (1998).
9. D. R. Alessi, A. Cuenda, P. Cohen, D. T. Dudley, A. R. Saltiel, *J. Biol. Chem.* **270**, 27489 (1995).
10. Cycling extracts were prepared from electrically activated *Xenopus* eggs as described [A. W. Murray and M. W. Kirschner, *Nature* **339**, 275 (1989); A. W. Murray, *Methods Cell Biol.* **36**, 581 (1991)]. To inhibit MEK activation, a dimethyl sulfoxide (DMSO) solution of PD98059 (Calbiochem) was added to yield a final concentration of 200 μM PD98059 and 1% DMSO. Control extracts were treated with DMSO alone. Immunodepletion of MEK was accomplished by incubating extracts for 75 to 90 min at 4°C with protein A–purified antibody 662 [K.-M. Hsiao, S.-y. Chou, S.-J. Shih, J. E. Ferrell Jr., *Proc. Natl. Acad. Sci. U.S.A.* **91**, 5480 (1994)] prebound to protein A–Sepharose beads (Sigma). Mock depletions were carried out with rabbit immunoglobulin G (IgG) in place of antibody 662.
11. MEK function appears to be essential for mitotic fragmentation of the Golgi apparatus in normal rat kidney cells [U. Acharya, A. Mallabiabarrena, J. K. Acharya, V. Malhotra, *Cell* **92**, 183 (1998)]. We were unable to assess the status of the Golgi apparatus because it is not well organized in extracts even in interphase.
12. This concentration of sperm (500 sperm per microliter) is substantially lower than that needed to reconstitute the spindle assembly checkpoint (about 9000 sperm per microliter) (*6*).
13. Activation of p42 MAPK can have various effects on cell cycle progression in *Xenopus* egg extracts, depending on when the activation occurs. When MAPK is activated early in the cycle, the result is a G_2-like arrest, with Cdc2–cyclin complexes present but inactive. When MAPK is activated just before mitosis, the result is arrest in a mitotic state with cyclin destruction partially inhibited—the classic cytostatic factor arrest [A. Abrieu, D. Fisher, M. N. Simon, M. Doree, A. Picard, *EMBO J.* **16**, 6407 (1997); S. A. Walter, T. M. Guadagno, J. E. Ferrell Jr., *Mol. Biol. Cell* **8**, 2157 (1997); J. C. Bitangcol *et al.*, *ibid.* **9**, 451 (1998); M. S. Murakami and G. F. Vande Woude, *Development* **125**, 237 (1998)].
14. N. Yew, M. L. Mellini, G. F. Vande Woude, *Nature* **355**, 649 (1992).
15. T. M. Guadagno and J. E. Ferrell Jr., unpublished data.
16. A. A. Reszka, R. Seger, C. D. Diltz, E. G. Krebs, E. H. Fischer, *Proc. Natl. Acad. Sci. U.S.A.* **92**, 8881 (1995).
17. To prepare interphase extracts, we incubated eggs with cycloheximide (100 μg/ml) at room temperature for 10 min, electrically activated them, and then packed and crushed them in the presence of cycloheximide [C. Smythe and J. W. Newport, *Methods Cell Biol.* **35**, 449 (1991)]. The resulting extracts were devoid of detectable cyclins and Mos and contained inactive p42 MAPK.

18. S. J. Mansour, J. M. Candia, J. E. Matsuura, M. C. Manning, N. G. Ahn, *Biochemistry* **35**, 15529 (1996).
19. The microtubule nucleation assay was done essentially as described [T. Stearns and M. Kirschner, *Cell* **76**, 623 (1994)]. Briefly, rhodamine-labeled bovine tubulin (from T. Stearns, Stanford University) and *Xenopus* sperm were added to extracts to yield final concentrations of 120 μg/ml and 200 nuclei per microliter, respectively. Extracts were incubated at room temperature for 10 min. Samples were diluted in 9 vol of glutaraldehyde (0.25%), centrifuged through a 25% glycerol cushion onto coverslips, and stained with DAPI. The DAPI-stained sperm and rhodamine-labeled tubulin were examined by fluorescence microscopy.
20. Addition of purified *Xenopus* or rat MAPK to interphase extracts can be sufficient to produce mitotic-like microtubules under some circumstances [Y. Gotoh *et al.*, *Nature* **349**, 251 (1991)]. One difference between their experiment and ours is the way the interphase extracts were prepared. We used cycloheximide-soaked eggs, and prepared the interphase extracts in cycloheximide-containing buffers, which prevents cyclin synthesis (*17*). Apparently they prepared interphase extracts in the absence of cycloheximide, and as a result their extracts may have contained substantial amounts of cyclins. The mitotic-like microtubules they observed therefore may have resulted from a combination of MAPK and Cdc2–cyclin activities.
21. N. Furuno *et al.*, *EMBO J.* **13**, 2399 (1994).
22. M. H. Verlhac *et al.*, *Development* **122**, 815 (1996).
23. Supported by a grant from the National Institutes of Health (GM46383). We thank T. Stearns for providing rhodamine-labeled tubulin and for advice; N. Ahn for providing MEK plasmids and for sharing unpublished data; G. Gorbsky and M. Weber for sharing unpublished data; M. Murakami and G. Vande Woude for providing Mos plasmids; and K. Cimprich and members of the Ferrell laboratory for comments on the manuscript. T.M.G. is a Special Fellow of the Leukemia Society of America. J.E.F. is a Howard Hughes Junior Faculty Scholar.

6 July 1998; accepted 14 October 1998

Catalytic Plasticity of Fatty Acid Modification Enzymes Underlying Chemical Diversity of Plant Lipids

Pierre Broun,* John Shanklin,*† Ed Whittle, Chris Somerville†

Higher plants exhibit extensive diversity in the composition of seed storage fatty acids. This is largely due to the presence of various combinations of double or triple bonds and hydroxyl or epoxy groups, which are synthesized by a family of structurally similar enzymes. As few as four amino acid substitutions can convert an oleate 12-desaturase to a hydroxylase and as few as six result in conversion of a hydroxylase to a desaturase. These results illustrate how catalytic plasticity of these diiron enzymes has contributed to the evolution of the chemical diversity found in higher plants.

All higher plants contain one or more oleate desaturases that catalyze the O_2-dependent insertion of a double bond between carbons 12 and 13 of lipid-linked oleic acid ($18:1^{\Delta 9}$) to produce linoleic acid ($18:2^{\Delta 9,12}$) (*1*). In contrast, only 14 species in 10 plant families have been found to accumulate the structurally related hydroxy fatty acid, ricinoleic acid (D-12-hydroxyoctadec-*cis*-9-enoic acid) (*2*), which is synthesized by an oleate hydroxylase that exhibits a high degree of sequence similarity to oleate desaturases (*3*). The oleate desaturases and hydroxylases are integral membrane proteins, which are members of a large family of functionally diverse enzymes that includes alkane hydroxylase, xylene monooxygenase, carotene ketolase, and sterol methyloxidase (*1*). These nonheme iron–containing enzymes use a diiron cluster for catalysis (*4*) and contain three equivalent histidine clusters that have been implicated in iron binding and shown to be essential for catalysis (*1*). This class of proteins exhibits no significant sequence identity to the soluble diiron-containing enzymes which represent a similar diversity of enzymatic activities that include plant acyl-ACP desaturases, methane monooxygenase, propene monooxygenase, and the R2 component of ribonucleotide reductase (*1*, *5*). The catalytic activities of these enzymes has been mimicked by a synthetic diiron-containing complex with a coordination sphere composed entirely of nitrogen ligands (*6*).

The oleate hydroxylase from the crucifer *Lesquerella fendleri* has about 81% sequence identity to the oleate desaturase from the crucifer *Arabidopsis thaliana* and about 71% sequence identity to the oleate hydroxylase from *Ricinus communis* (*7*). The observation that these crucifer desaturase and hydroxylase enzymes are more similar than the two hydroxylases, and the presence of ricinoleic acid in a small number of distantly related plant species, suggests that the capacity to synthesize ricinoleate has arisen independently several times during the evolution of higher plants, by the genetic conversion of desaturases to hydroxylases.

Comparison of the amino acid sequences of the hydroxylases from *L. fendleri* and *R. communis* with the sequences for oleate desaturases from *Arabidopsis*, *Zea mays*, *Glycine max* (two sequences), *R. communis*, and *Brassica napus* revealed that only seven residues were strictly conserved in all of the six desaturases but divergent in both of the hydroxylases. The role of these seven residues was assessed by using site-directed mutagenesis to replace the residues found in the *Lesquerella* hydroxylase, LFAH12, with those from the equivalent positions in the desaturases (*8*, *9*). In a reciprocal experiment, we replaced the seven residues in the *Arabidopsis* FAD2 oleate desaturase with the corresponding *Lesquerella* hydroxylase residues (*10*). The activity of the modified and unmodified genes was then determined by expressing them in yeast and transgenic plants before analyzing the composition of the total fatty acids. Technical difficulties limited the utility of direct measurements of enzyme activity in cell extracts (*11*).

The mutant hydroxylase and desaturase genes containing all seven substitutions (designated m_7LFAH12 and m_7FAD2, respectively) were expressed in yeast cells under transcriptional control of the GAL1 promoter. Transgenic cells were harvested after induction and their total fatty acid composition determined by gas chromatography. Wild-type yeast cells do not accumulate detectable concentrations of diunsaturated or hydroxylated fatty acids (*12*). Expression of FAD2 caused the accumulation of about 4% diunsaturated fatty acids (16:2 and

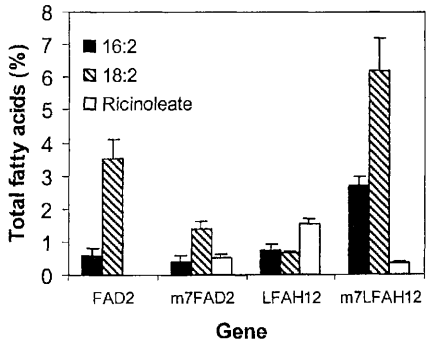

Fig. 1. Fatty acid composition of yeast cells expressing desaturase and hydroxylase genes. Cultures were induced in growth medium containing galactose, ~2 × 10^8 cells were harvested, and fatty acids were extracted and modified for analysis by gas chromatography, as described (*7*). Values are the averages (±SE) obtained from five cultures of independent transformants.

P. Broun and C. Somerville, Carnegie Institution of Washington, Department of Plant Biology, 260 Panama Street, Stanford, CA 94305, USA. J. Shanklin and E. Whittle, Biology Department, Brookhaven National Laboratory, Upton, NY 11973, USA.

*These authors contributed equally to this work.
†To whom correspondence should be addressed.